Received: 11 March 2022 | Revised: 26 May 2022 | Accepted: 29 June 2022

DOI: 10.1002/psp4.12847

ARTICLE

Physiologically-based pharmacokinetic modeling of immunoglobulin and antibody coadministration in patients with primary human immunodeficiency

Sara N. Salerno[1] | **Rong Deng**[1,2] | **Tarundeep Kakkar**[1]

[1]Gilead Sciences, Inc., Foster City, California, USA

[2]R&D Q-Pharm Consulting LLC, Pleasanton, California, USA

Correspondence
Sara N. Salerno, Gilead Sciences, Inc, 310 Lakeside Drive, Foster City, CA 94404, USA.
Email: sara.salerno1@gilead.com

Abstract

Intravenous immunoglobulin (IVIG) (2000 mg/kg) increased the clearance of the mouse monoclonal antibody 7E3, directed against platelet integrin IIb/IIIa (alpha IIb beta 3, CD41/CD61) in rodents. We wanted to investigate the effect of IVIG on clearance of monoclonal antibodies in humans as there is extremely limited data regarding this interaction in the literature. Using the tyrosine protein kinase KIT anti-cluster of differentiation 117 (c-Kit) humanized monoclonal antibody (JSP191) as a case study, we used physiologically-based pharmacokinetic (PBPK) modeling to evaluate the pharmacokinetic interaction between monoclonal antibodies and IVIG at doses (300–600 mg/kg) administered to patients with primary human immunodeficiency (PI). We first characterized the interaction between monoclonal antibodies and IVIG in PK-Sim®/MoBi® using published literature data, including the following: IVIG plus 7E3 in mice and rats and IVIG plus the human anti-C5 monoclonal antibody tesidolumab in adults with end-stage renal disease. We next developed a PBPK model using digitized data for JSPI91 alone in older adults with myelodysplastic syndrome and acute myeloid leukemia and in pediatric patients with severe combined immunodeficiency (SCID). Finally, we simulated the impact of IVIG (300–2000 mg/kg) coadministration with JSP191 on the area under the curve of JSP191 in patients with SCID. Model predictions were within 1.5-fold of observed values for 7E3 plus IVIG and tesidolumab plus IVIG as well as for JSP191 administered alone. Based on our simulations, IVIG doses ≥500 mg exceeded the 80%–125% no-effect boundaries. IVIG treatment with monoclonal antibodies in patients with PI may result in a clinically significant interaction depending on the IVIG dose administered and the exposure–response relationship for the specific monoclonal antibody.

Study Highlights

WHAT IS THE CURRENT KNOWLEDGE ON THE TOPIC?

In mice and rats, high doses (1000–2000 mg/kg) of intravenous immunoglobulin (IVIG) pretreatment significantly increased clearance of the monoclonal antibody

(7E3) directed against platelet integrin IIb/IIIa (alpha IIb beta 3, CD41/CD61) due to competition of binding to the neonatal fragment crystallizable-receptor.

WHAT QUESTION DID THIS STUDY ADDRESS?

There is extremely limited clinical information describing the interaction between monoclonal antibody and IVIG treatment. This study leveraged physiologically-based pharmacokinetic (PBPK) modeling to characterize whether lower doses of IVIG (300–600 mg/kg) administered to patients with primary humoral immunodeficiency may lead to a significant pharmacokinetic interaction with monoclonal antibodies.

WHAT DOES THIS STUDY ADD TO OUR KNOWLEDGE?

Based on our simulations using the humanized monoclonal antibody against c-Kit (JSP191) as a case study, the 90% confidence intervals for JSP191 in combination with IVIG at doses ≥500 mg/kg relative to JSP191 alone exceeded the default no-effect boundary of 80%–125%.

HOW MIGHT THIS CHANGE DRUG DISCOVERY, DEVELOPMENT, AND/OR THERAPEUTICS?

IVIG doses ≥500 mg/kg with monoclonal antibodies may result in a significant drug–drug interaction (DDI). PBPK modeling could characterize the DDI potential for large molecules.

INTRODUCTION

Intravenous immunoglobulin (IVIG) therapy is administered to patients with autoimmune and inflammatory diseases, such as idiopathic thrombocytopenic purpura, chronic inflammatory demyelinating polyneuropathy, and primary humoral immunodeficiency (PI). PI is a heterogenous group of disorders of the immune system including congenital agammaglobulinemia, common variable immunodeficiency, X-linked agglamaglobulinemia, Wiscott-Aldrich syndrome, and severe combined immunodeficiency (SCID). The immunoregulatory effects of IVIG are complex and involve the blockade of fragment crystallizable region (Fc) gamma receptor macrophages and effector cells. Binding of IVIG to the protective neonatal Fc receptor (FcRn) in endocytotic vesicles may also accelerate the clearance (CL) of immunoglobulin G (IgG) and reduce pathogenic antibodies.[1]

High-dose IVIG increases the CL of IgG monoclonal antibodies through saturation of the pH-dependent binding of IgG to FcRn, which is expressed primarily in endothelial and myeloid cells. FcRn protects IgG from lysosomal degradation by first binding IgG in the acidic endosome after fluid-phase endocytosis, recycling IgG back to the cell surface, and then releasing IgG in the serum at physiological pH.[2] In rats, IVIG pretreatment (0, 400, 1000, and 2000 mg/kg) resulted in a dose-dependent increase in CL of the monoclonal antibody (7E3) directed against platelet integrin IIb/IIIa (alpha IIb beta 3, CD41/CD61) and resulted in a significant change in the degree and time course of 7E3-induced thrombocytopenia.[3] In mice, 1000 mg/kg IVIG increased 7E3 CL from 5.2 ± 0.3 to 14.4 ± 1.4 ml/day/kg.[4,5]

To our knowledge, only two clinical studies have reported pharmacokinetic (PK) changes associated with IVIG and monoclonal antibody therapy in humans. In one study, eight adult patients with end-stage renal disease awaiting kidney transplantation were assigned to receive a single dose (20 mg/kg) of tesidolumab, a recombinant human IgG1/lambda monoclonal antibody against the human C5 complement cascade, alone or after 2000 mg/kg IVIG treatment. The mean tesidolumab exposure decreased by 34%, and CL increased by 63% in the six patients receiving tesidolumab plus IVIG relative to the two patients receiving tesidolumab alone. In addition, complete suppressions of total and alternative complement activities were lower for the tesidolumab plus IVIG group (2 weeks) relative to the tesidolumab-alone group (4 weeks).[6] In another study, a population PK model was developed for infliximab in 70 children (median [interquartile range] 2.9 years of age [1.3–4.4 years of age]) receiving infliximab (5 mg/kg) as adjunctive therapy with 2000 mg/kg IVIG for acute Kawasaki disease. The authors concluded that administering infliximab after IVIG, as opposed to before, resulted in a 50% decrease in the peripheral volume of infliximab.[7]

In patients with PI, IVIG is administered at 300–600 mg/kg every 3–4 weeks. The objective of this study was to leverage physiologically-based PK (PBPK) modeling to explore whether coadministration of monoclonal antibodies with lower IVIG doses results in a significant interaction using the humanized monoclonal antibody (JSP191) that binds human cluster of differentiation 117 (c-Kit) as a case study. JSP191 is under investigation as a nontoxic conditioning regimen for hematopoietic stem

cell transplantation in patients with SCID, myelodysplastic syndrome (MDS), acute myeloid leukemia (AML), and sickle cell disease.[8–11] In this study, we (1) developed and evaluated the interaction between IVIG and monoclonal antibodies in PK-Sim®/MoBi® (Open Systems Pharmacology) using digitized published data for 7E3 plus IVIG in rodents[3,4] and tesidolumab plus IVIG in adults[6] (model validation), (2) developed an adult and pediatric PBPK model for JSP191 using published digitized data (base model for JSP191),[8–10] and (3) simulated the impact of IVIG (300–2000 mg/kg) coadministration with JSP191 on the area under the curve (AUC) and CL of JSP191 in virtual pediatric and adult patients with SCID (Figure S1).

METHODS

Software

Physiologically-based pharmacokinetic modeling was performed using the open source software, PK-Sim®/MoBi®, Version 9.1 (https://www.open-systems-pharmacology.org/).[12] The PBPK model for proteins was developed and validated as an extension of the model for small molecules and incorporates the two-pore formalism for drug extravasation from blood plasma to interstitial space, lymph flow, endosomal CL, and protection from endosomal CL through FcRn binding (Supplemental Information S1).[13] Endogenous IgG is included in the model as one compartment to allow for physiological steady-state conditions prior to drug administration and consists of plasma, interstitial, and endosomal space substructures. A zero-order synthesis of endogenous IgG continuously releases endogenous IgG into the plasma space to account for loss of endogenous IgG not bound to FcRn in the endosomal space. The equations for the steady-state concentration of endogenous IgG, FcRn, and endogenous IgG-FcRn complex without drug are used as initial conditions.[13] Both endogenous and exogenous IgG compete with the monoclonal antibody (drug) for binding to the FcRn receptor within the simulations. Drug and endogenous IgG can reversibly bind to FcRn forming a FcRn complex in the plasma and interstitial space with low affinity and within the endosomal space with high affinity (dissociation constant [K_d] set to 999,999 µM, resulting in essentially no binding to FcRn). Equations for the mass transfer of the drug and endogenous IgG to the endosomal space, recycling of the FcRn complex, specific CL of drug or endogenous IgG not bound to FcRn, and FcRn binding for the drug and endogenous IgG are provided in the Supplemental Information S1.[13] More information on the model code is provided in Supplemental Information S2. All of the plasma PK data that were used in this study for model evaluation were extracted from the literature and digitized using the online software WebPlotDigitizer Version 4.5 (https://automeris.io/WebPlotDigitizer/index.html).

PBPK model for 7E3 plus IVIG in mice and rats

We simulated the effect of IVIG on the PK of 7E3 in mice using a previously published mouse model for 7E3 (Table 1) and then compared the simulations to the observed plasma concentration versus time data that were reported for 7E3 in mice receiving an intravenous (i.v.) bolus of 8 mg/kg with and without 1 g/kg of IVIG.[4,13] Population simulations were performed for 100 mice (18–35 g) with an assumed variability of 25% introduced on plasma IgG concentrations. Simulations were also performed for 7E3 in rats and then compared with observed data reported in female Sprague–Dawley rats (200–225 g) receiving 7E3 (8 mg/kg) with and without IVIG pretreatment (0, 0.4, 1, and 2 g/kg).[3] The plasma endogenous IgG concentrations were changed to the reported value in rats of 60 µM, and then the rate constant for endosomal uptake was optimized to 0.80 1/min using the control rat data (no IVIG) with the Monte Carlo algorithm (Supplemental Information S2).[14,15]

TABLE 1 Final drug parameters

Parameter	7E3	IVIG	Tesidolumab	JSP191
Molecular weight (kDa)	150[13]	149[37]	150	145
Hydrodynamic radius (nm)	5.34[13]	5.34[13]	5.34[13]	5.34[13]
FcRn binding affinity in the endosome (K_d) (nM)	750[13]	630[37]	727[38]	727[38]
CD117 (c-Kit) dissociation constant (K_d) (nM)	n/a	n/a	n/a	0.0141[a]
c-Kit degradation rate (1/h)	n/a	n/a	n/a	0.23[39]
JSP191-CD117 (c-Kit) internalization rate (1/h)	n/a	n/a	n/a	5.40[39]

Abbreviations: FcRn, neonatal fragment crystallizable-receptor; IVIG, intravenous immunoglobulin; K_d, dissociation constant; n/a, not applicable.

[a]Optimized using adult data.

PBPK model for tesidolumab plus IVIG in adults

A PBPK model for IVIG was previously developed in healthy adult subjects.[16] The tesidolumab model was developed and evaluated using observed data in eight adult patients (18–70 years of age) on chronic dialysis with end-stage renal disease awaiting kidney transplantation. In this study, six patients with a mean age of 54.7 years received 2000 mg/kg IVIG treatment (up to a maximum dose of 140 g) followed by a single dose of 20 mg/kg tesidolumab, and two patients (mean age of 49.0 years) received a single dose of 20 mg/kg tesidolumab. Half of these eight subjects were White.[6] Information regarding the administration schedule was not provided, so we assumed a 60-min infusion time for tesidolumab as the observed maximum concentration (C_{max}) after dosing was around 1 h post dose, and the infusion rate for IVIG was based on recommendations in the package insert for chronic inflammatory demyelinating polyneuropathy (starting at 2 mg/kg/min for 30 min and increasing to 8 mg/kg/min as tolerated; Supplemental Information S1).[17] Using PK data for tesidolumab alone, the rate constant for endosomal uptake was optimized in a virtual White American male (50 years of age) to 0.33 1/min using the Monte Carlo algorithm. Population simulations were generated for 100 White American virtual subjects based on demographics from the underlying population: 33% female, 30–65 years of age, a mean body mass index of 30 kg/m^2, and a plasma IgG concentration ranging from 50 to 167 μM.[6]

Adult and pediatric PBPK model for JSP191

An adult PBPK model was first developed for JSP191 to determine key parameters before scaling to pediatric patients. The model was developed and evaluated using observed data collected in six older adults (83% male) with AML/MDS who had a mean (range) age of 70 years (65–74 years) and who received a single dose of 0.6 mg/kg JSP191.[8] A 70-year-old virtual White American male was used for model development with binding to c-Kit, and c-Kit expression was taken from the built-in gene database query that determines protein abundances based on relative tissue-specific expression data from publicly available sources.[18] The relative expressions for the c-Kit protein were used based on whole genome expression arrays from Array Express and were localized on the extracellular matrix (Table S1).[12]

The adult PBPK model was first developed in PK-Sim® and then exported to MoBi® to account for target-mediated drug disposition (TMDD) via the internalization of the c-Kit/JSP191 complex. The synthesis and degradation of c-Kit were incorporated as a function of the amount of receptor and the rate of synthesis/degradation. The rate of synthesis and degradation of c-Kit were assumed to be the same, thereby assuming no buildup or loss of receptors over time at steady state. The internalization was incorporated as a function of the amount of JSP191–c-Kit complex and the internalization rate. The amount of c-Kit can be calculated as a product of the relative expression of c-Kit in each organ/tissue (Table S1), the reference concentration, the ontogeny factor (set to 1), and the volume of each organ/tissue. The reference concentration represents the protein expression relative to the expression in the organ with highest concentration of the respective enzyme. The reference concentration of c-Kit was optimized to 457 pmol/L, and the K_d for c-Kit was optimized using the Monte Carlo algorithm because these parameters were not reported (Table 1). Population simulations in 100 virtual White American adults from 65 to 74 years of age (83% male) were generated for model evaluation.

The virtual White American male (70 years of age) was scaled to a virtual child (12 years of age) based on the age dependencies of relevant physiological parameters (body weight, height, organ weights, blood flows, interstitial space, and vascular space) as previously described.[19] The pediatric model was developed and evaluated using observed data from a phase I trial in four retransplanted children and adults (11, 12, 12, 38 years of age) with SCID receiving 0.3 mg/kg JSP191.[10] Target-mediated disposition based on the optimized c-Kit levels in AML/MDS resulted in a significant underprediction of CL of JSP191 in the SCID population, so the c-Kit concentration was optimized to 1873 pmol/L using observed JSP191 PK data in patients with SCID.

Drug–drug interaction simulations between JSP191 and IVIG

Based on a literature review, the CL of IVIG in patients with PI were approximately 2–3 times lower than in healthy adults (Table S2). To account for these differences, the rate constant for endosomal uptake was optimized to 0.13/min (default value was 0.29/min) (Table S2). We next simulated JSP191 (a single dose of 0.3 mg/kg over a 60-min infusion) in combination with 0, 300, 400, 500, 600, 1000, and 2000 mg/kg IVIG to evaluate the impact of IVIG dosing on JSP191 CL. Based on a systematic review in 1218 patients with PI receiving mean IVIG doses from 387 to 560 mg/kg every 3–4 weeks, the IgG baseline levels ranged from 660 to 1280 mg/dl.[20] Therefore, we changed the default endogenous plasma IgG value in PK-Sim® from 1043 mg/dl to a uniform range from 660 to 1280 mg/dl in all of the population simulations of 100 virtual patients with SCID from 11 to 38 years of age (50% male) (Figure S2).

Model validation

To evaluate model performance, concentration versus time plots were plotted comparing the simulated mean and associated 90% prediction interval to the observed data. The average fold error (AFE) was calculated comparing the simulated geometric mean with the observed data for each available concentration-time point according to Equation (1):

$$\mathrm{AFE} = 10^{\left(\frac{1}{n}\right) * \sum \log\left(\frac{\text{predicted}}{\text{observed}}\right)} \quad (1)$$

In addition, we calculated the percentage of model-predicted to observed plasma concentrations and the ratio of predicted to observed PK parameters within the twofold prediction error (0.5- to 2-fold) and the 1.5-fold prediction error (0.667- to 1.5-fold). Model performance was considered acceptable if all predictions were within the twofold prediction error and most within the 1.5-fold prediction error.

RESULTS

7E3 plus IVIG in mice and rats

The PBPK model predictions for 7E3 with and without IVIG treatment were comparable with observed data in mice receiving 8 mg/kg 7E3 IV plus 1000 mg/kg IVIG bolus dosing (Figure S3).[3] The AFE for the predicted/observed concentrations and the predicted to observed mean CL ratios for 7E3 in mice were all within the 1.5-fold prediction error (Table 2). In rats, the PBPK model simulations slightly underpredicted CL for 7E3 plus 0.4 g/kg IVIG and slightly overpredicted CL for 7E3 plus 1 and 2 g/kg IVIG (Table 2, Figure S4). However, the predicted to observed mean CL ratios for 7E3 in rats were all within the 1.5-fold prediction error (Table 2). There was also model misspecification for the 7E3 concentrations during the early timepoints (within the first day of treatment) that is likely attributed to difficulties discerning these points on the published plot used to digitize the data (Figure S4).

Tesidolumab plus IVIG in adults

The PBPK model for IVIG was previously developed and evaluated in healthy adults (Figure S5).[16] The tesidolumab model slightly overpredicted tesidolumab concentrations with an AFE for predicted to observed concentrations of 1.29 for tesidolumab and 1.18 for tesidolumab plus IVIG (Figure 1). The predicted PK parameters (AUC to last observation [AUC_{last}], AUC extrapolated to infinity [AUC_{∞}], C_{max}, and CL) were all within the 1.5-fold prediction error except for C_{max} for tesidolumab plus 2000 mg/kg IVIG, which was slightly higher but still within the twofold prediction error (Table 3). The predicted and observed geometric mean ratios and associated 90% confidence intervals of C_{max}, AUC_{last}, and AUC_{∞} for tesodolumab plus 2000 mg/kg IVIG relative to tesidolumab alone were also comparable between the observed and simulated parameters and within the 1.5-fold prediction error, albeit with higher variability in the subjects with end-stage renal disease relative to the virtual population (Table 3).

TABLE 2 Comparison of observed and simulated clearance for 7E3 (8 mg/kg i.v. bolus) with and without IVIG treatment in mice and rats

Dose of IVIG, mg/kg	Observed mean clearance of 7E3, ml/h/kg	Simulated clearance of 7E3, ml/h/kg	Simulated to observed mean clearance ratio	AFE for simulated/observed concentrations
Mouse				
0	0.22	0.21	0.95	1.08
1000	0.60	0.68	1.13	0.93
Rat				
0	0.78	0.77	0.99	1.00
400	1.28	1.10	0.86	1.17
1000	1.37	1.60	1.17	0.94
2000	1.85	2.30	1.24	0.89

Note: Observed data are presented as the mean clearance for 7E3, an antiplatelet antibody directed against platelet integrin IIb/IIIa (alpha IIb beta 3, CD41/CD61), with and without IVIG bolus dosing in three mice and in female Sprague–Dawley rats (200–225 g).[3,4] Simulated data are based on simulations for a virtual rat and virtual mice (sex unknown) in PK-Sim®/MoBi®. The AFE was calculated comparing the simulated mean with the observed data for each available concentration-time point as follows: $10^{\left(\frac{1}{n}\right) * \sum \log\left(\frac{\text{predicted}}{\text{observed}}\right)}$.

Abbreviations: AFE, average fold error; i.v., intravenous; IVIG, intravenous immunoglobulin.

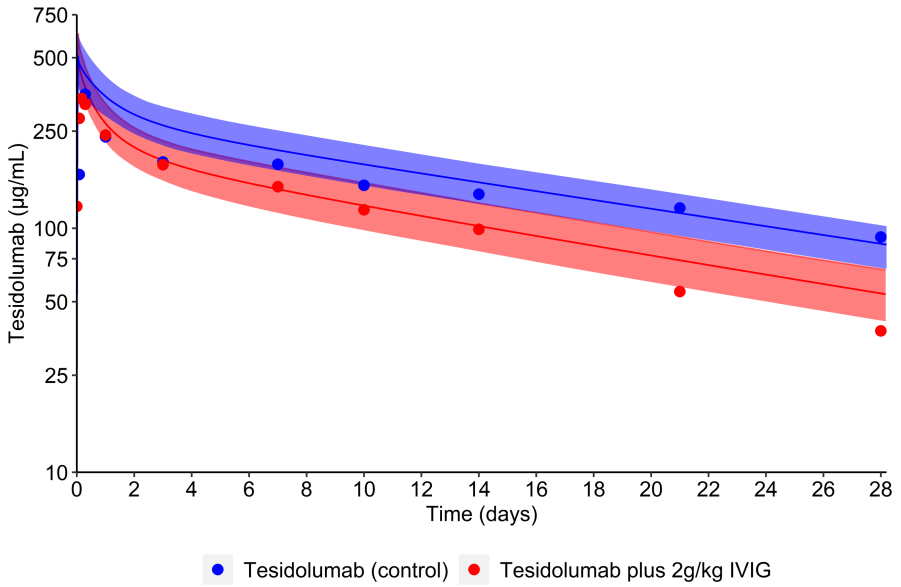

FIGURE 1 Adult population simulations for tesidolumab (20 mg/kg) administered with and without 2000 mg/kg intravenous immunoglobulin (IVIG). Population simulations were performed in 100 White American virtual subjects from 30 to 65 years of age receiving a single dose of tesidolumab (20 mg/kg over a 60-min infusion) with and without 2000 mg/kg of IVIG therapy. Simulated data are presented as geometric mean (solid line) and associated 90% confidence interval (shaded area), where blue represents tesidolumab alone and red represents tesidolumab plus IVIG. Observed data were obtained from a study in eight adult patients (18–70 years of age) on chronic dialysis with end-stage renal disease awaiting kidney transplantation. In this study, six patients (mean age of 54.7 years) received 2000 mg/kg IVIG treatment followed by a single dose of 20 mg/kg tesidolumab, and two patients (mean age of 49.0 years) received a single dose of 20 mg/kg tesidolumab. Blood samples for pharmacokinetic analysis were collected on Day 1 at 0, 2, 4, 7 h and on Days 2, 4, 8, 11, 15, 22, 29, and 57 post tesidolumab dosing.[6]

TABLE 3 Comparison of observed and simulated PK parameters for tesidolumab (20 mg/kg) with and without 2000 mg/kg IVIG in adult patients with end-stage renal disease

PK parameter	AUC_{last} (day*μg/ml)	AUC_{∞} (day*μg/ml)	C_{max} (μg/ml)	CL (L/h)
Observed				
Tesidolumab, mean ± SD	5780 ± 1060	6600 ± 1660	367 ± 81.3	0.0120 ± 0.00031
Tesidolumab plus 2000 mg/kg IVIG, mean ± SD	3540 ± 502	3680 ± 449	319 ± 50.7	0.0196 ± 0.00517
Geometric mean ratio (90% CI)	0.612 (0.48, 0.78)	0.563 (0.44, 0.71)	0.871 (0.66, 1.15)	1.63 (n/a)
Simulated				
Tesidolumab, mean ± SD	4916 ± 514	6917 ± 752	506 ± 70.4	0.0102 ± 0.00156
Tesidolumab plus 2000 mg/kg IVIG, mean ± SD	3379 ± 436	4612 ± 628	502 ± 69.6	0.0154 ± 0.00296
Geometric mean ratio (90% CI)	0.685 (0.673, 0.698)	0.664 (0.651, 0.678)	0.992 (0.992, 0.993)	1.50 (1.47, 1.54)

Note: PK parameters are presented as mean ± SD, and the fold changes for tesidolumab plus IVIG relative to tesidolumab alone are presented as the geometric mean ratio and associated 90% CI. Population simulations were performed in 100 White American virtual subjects. Observed data were reported in eight adult patients (18–70 years of age) on chronic dialysis with end-stage renal disease awaiting kidney transplantation, of which six received 2000 mg/kg IVIG treatment plus 20 mg/kg tesidolumab and two patients received a single dose of 20 mg/kg tesidolumab.[6]

Abbreviations: AUC_{last}, area under the curve from 0 to the last observation; AUC_{∞}, area under the curve from 0 to infinity; CI, confidence interval; C_{max}, maximum concentration; CL, clearance; IVIG, intravenous immunoglobulin; n/a, not applicable; PK, pharmacokinetic.

Adult and pediatric PBPK model for JSP191

We developed and evaluated a PBPK model for JSP191 in older adults with AML/MDS before scaling to pediatric patients. The AFE comparing the predicted and observed concentration versus time data in older adults with AML/MDS was well within the predetermined acceptance criteria of two-fold. This slight overprediction (i.e., >1.5-fold AFE) appears to be driven by one subject (Figure 2), but we did not have specific demographics for this subject. The PBPK model for JSP191 in pediatrics and young adults (11–38 years of age) with SCID characterized the PK data

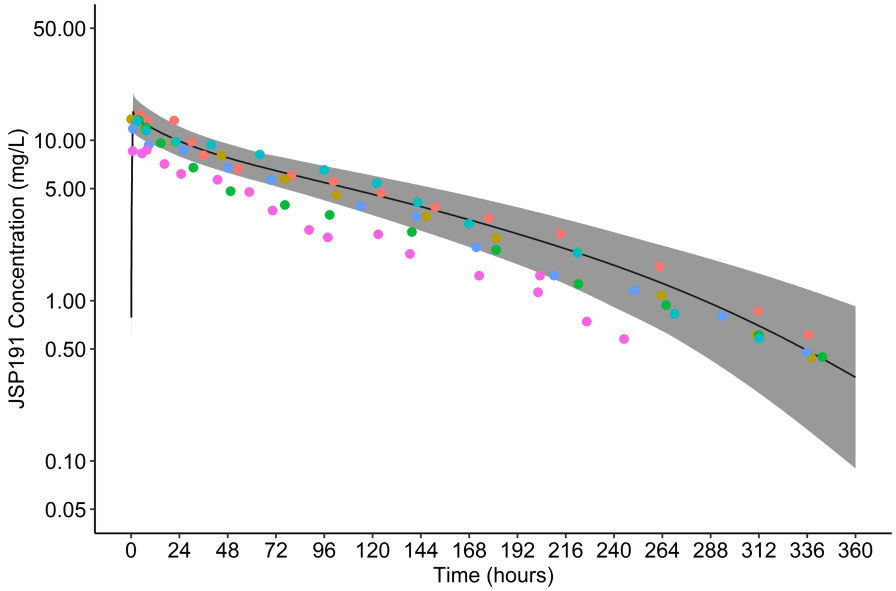

FIGURE 2 Population simulations for JSP191 (single intravenous infusion of 0.6 mg/kg) in older adults with myelodysplastic syndrome and acute myeloid leukemia. Population simulations were performed in 100 virtual White American adults from 65 to 74 years of age (83% male) receiving a single dose of intravenous 0.6 mg/kg JSP191 (60-min infusion). Simulated data are presented as geometric mean (solid black line) and associated 90% confidence interval (shaded gray area). Observed data were collected in six older adults (83% male) with myelodysplastic syndrome and acute myeloid leukemia with a mean (range) age of 70 (65–74) years who received a single dose of 0.6 mg/kg JSP191.[8]

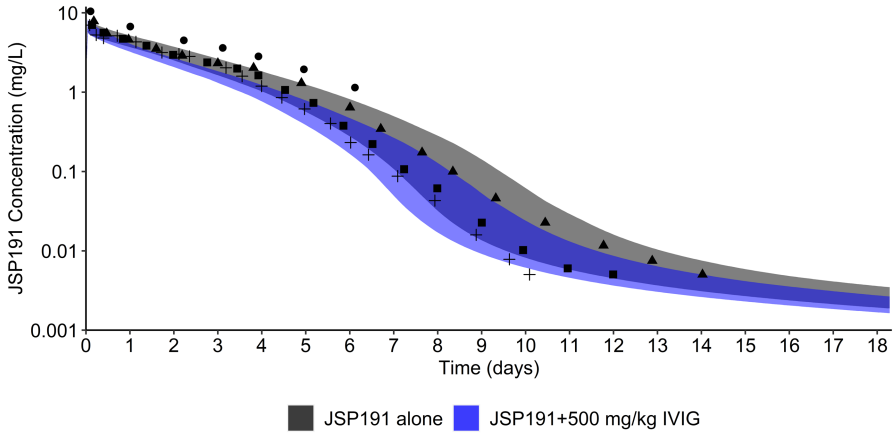

FIGURE 3 Population simulations for JSP191 (0.3 mg/kg) administered with and without 500 mg/kg intravenous immunoglobulin (IVIG) therapy in patients with severe combined immunodeficiency disorders. Population simulations were performed in 100 virtual children and young adults from 11 to 38 years of age (50% male) receiving JSP191 (a single dose of 0.3 mg/kg over a 60-min infusion) alone (shaded black area is the simulated 90% confidence interval) or in combination with 500 mg/kg of IVIG (blue shaded area is the simulated 90% confidence interval). The observed data were obtained from a phase I trial in four retransplanted children and adults with severe combined immunodeficiency disorders (11, 12, 12, and 38 years of age) whom received 0.3 mg/kg of JSP191. Observed data are stratified by shape representing data from individual subjects.[10]

well, with an AFE comparing the predicted and observed concentration versus time data for JSP191 administered alone of 1.05 (Figure 3). The simulated mean (range) CL of JSP191 was 0.0136 (0.0065–0.0209) ml/min/kg in virtual children (10–13 years of age) and was 0.0130 (0.0072–0.0211) in virtual adults (18–38 years of age) (Figure S6). We simulated the concentration of JSP191 at doses (0.1, 0.3, 1, and 3 mg/kg) in a virtual 12-year-old child with SCID and compared with the only digitized observed data available at 0.3 mg/kg to characterize the TMDD (Figure S7). There was one subject with slightly higher concentrations, but we did not have specific demographic information for this individual. It is also likely that these individuals were receiving IVIG therapy to prevent infections, but we did not have any information regarding the dose or timing of IVIG administration relative to JSP191.

Therefore, we compared simulations with and without 500 mg/kg IVIG coadministration (Figure 3).

Drug–drug interaction simulations between JSP191 and IVIG in pediatric patients with SCID

We simulated JSP191 with 300–2000 mg/kg IVIG in 100 virtual subjects from 11 to 38 years of age and calculated the geometric mean fold ratios for C_{max}, CL, and AUC_{∞} relative to JSP191 administered alone. As expected, there was no change in C_{max}, but there was a dose-dependent increase in CL and a decrease in AUC_{∞} (Table S3 and Figure 4). Using the Food and Drug Administration (FDA) guidelines for interpreting drug–drug interaction (DDI) studies in the absence of an exposure–response relationship, we calculated the geometric mean ratios and associated 90% confidence intervals for systemic exposure ratios of JSP191 in combination with IVIG relative to JSP191 alone.[21] The simulated 90% confidence interval for IVIG at doses ≥500 mg/kg exceeded the default no-effect boundary of 80%–125% (Figure 4). We did not observe any differences in this interaction when the data were stratified by age: <18 years of age versus 18–38 years of age (Table S3). If we removed TMDD (lacking c-Kit as a binding partner), the magnitude of the DDI for JSP191 was even greater and the simulated 90% confidence interval exceeded the no-effect boundary for IVIG at lower doses (≥300 mg/kg) (Table S4). The effect of endogenous IgG had a small impact; the simulated ratio (90% confidence interval) for AUC_{∞} was 0.48 (0.48–0.49) versus 0.43 (0.42–0.43) in pediatric patients with SCID with endogenous IgG levels of 1043 mg/dl (default) versus 500 mg/dl, respectively.

DISCUSSION

Physiologically-based pharmacokinetic modeling is routinely used during drug development to predict metabolism and transporter-mediated DDI potential for small molecules, but it is less frequently applied for biologics. Recently, PBPK models have been developed to predict cytokine and disease–drug interactions for antibodies.[22–26] For example, PBPK modeling evaluated the impact of transient elevations of interleukin-6 by the CD19/CD3 bispecific T cell engager, blinatumomab, on hepatic cytochrome P450 activities.[25] There have also been a few published PBPK models that characterized DDIs for antibodies due to FcRn competition. A published minimal PBPK model predicted that treatment with the anti-CD38 antibody, daratumumab, for multiple myeloma resulted in a 3.6-fold increase in the daratumumab half-life following M-protein reduction, which was mediated by paraprotein competition with FcRn binding.[27] In addition, a mouse PBPK model demonstrated that IVIG (1000 mg/kg) increased 7E3 CL in control but not FcRn knockout mice.[3] However, there is extremely limited clinical information characterizing the DDI between IVIG and monoclonal antibodies in humans.

We leveraged PBPK modeling to evaluate whether coadministration of monoclonal antibodies with moderate doses of IVIG (300–600 mg/kg every 3–4 weeks) administered to patients with PI results in a significant interaction

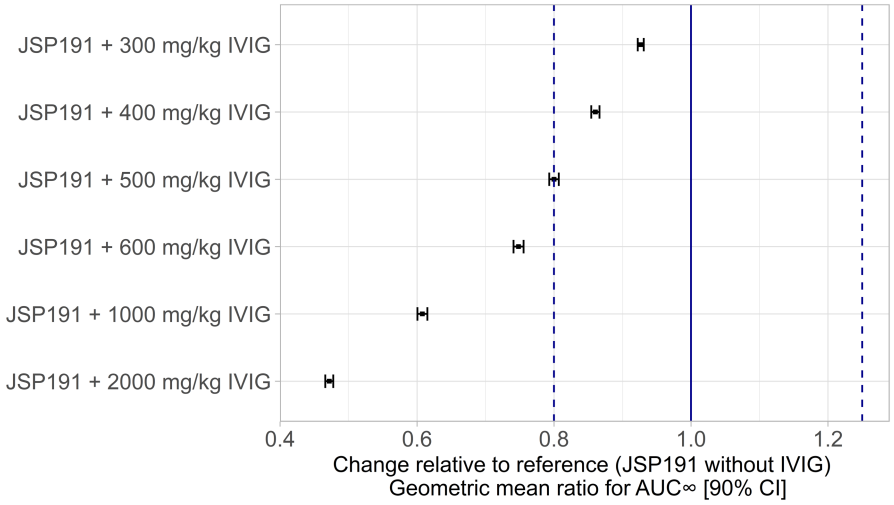

FIGURE 4 Simulated change in the area under the curve extrapolated to infinity (AUC_{∞}) for JSP191 plus intravenous immunoglobulin (IVIG) (300–2000 mg/kg) in virtual subjects (11–38 years of age) with severe combined immunodeficiency disorders. Population simulations were performed in 100 virtual children and young adults from 11 to 38 years of age (50% male) receiving JSP191 (a single dose of 0.3 mg/kg over a 60-min infusion) alone or in combination with 300, 400, 500, 600, 1000, and 2000 mg/kg IVIG therapy. Data are presented as geometric mean ratio for the AUC_{∞} for JSP191 plus IVIG relative to JSP191 alone. CI, confidence interval.

using JSP191 as a case study (Figure S1). We used the open-source software PK-Sim®/MoBi® because of accessibility and ease of use, which may be useful to predict DDI potential for other monoclonal antibodies under clinical development that may be coadministered with IVIG. We first developed and evaluated PBPK models with PK data available from the literature, including 7E3 plus IVIG in mice and rats and tesidolumab plus IVIG in adults with end-stage renal disease.[3,4,6] The PBPK model predictions for 7E3 plus IVIG and tesidolumab plus IVIG were comparable and within 1.5-fold of the observed values. Next, we developed and evaluated an adult and pediatric PBPK model for JSP191 based on published PK data available in older adults with AML/MDS and in patients with SCID.[8,10] Finally, we simulated the impact of IVIG (300–2000 mg/kg) coadministration with JSP191 on the AUC_{∞} and CL of JSP191 in virtual patients with SCID.

Hansen and Balthasar also published a PBPK model in mice for 7E3 plus 1000 mg/kg IVIG in control and FcRn knockout mice with predicted versus observed mean ± SD plasma AUC of 1320 versus 1460 ± 78.6 μg/ml day for 7E3 alone, 594.4 versus 488 ± 40.1 μg/ml day for 7E3 plus IVIG in control mice, and 108 versus 110 ± 6.8 μg/ml day in FcRn knockout mice.[3] This PBPK model had slightly different assumptions for FcRn-mediated recycling and endosomal CL than implemented within PK-Sim®/MoBi®. Hansen and Balthasar assumed that FcRn capacity in each tissue was proportional to tissue weight and was scaled in each tissue based on the estimated total body capacity of FcRn.[3] In PK-Sim®/MoBi®, FcRn concentration was assumed the same in each organ, but the endosomal uptake was proportional to the endosomal volume and the vascular volume in each organ.[13] In addition, the drug–FcRn binding reaction in PK-Sim®/MoBi® was explicitly represented in a simplified submodel allowing for different FcRn binding affinities for the drug and endogenous IgG.[13] In PK-Sim®/MoBi®, FcRn binding affinities differed between the acidic endosomal space and the neutral environment with a very high value (999,999 μM) in the neutral space, resulting in virtually no FcRn binding at neutral environments for all compounds. However, both the published and our developed PBPK models were able to capture concentration-time profiles of 7E3 in wild-type and FcRn knockout mice in the plasma, lung, kidney, skin, muscle, spleen, liver, heart, and gut reasonably well.[3,13]

After validating the predictive performance of monoclonal antibodies with IVIG in PK-Sim®/MoBi®, we simulated the interaction between IVIG with JSP191, a monoclonal antibody likely to be coadministered to patients receiving IVIG for the prevention of infections. We first developed and evaluated an adult PBPK model for JSP191 alone in older adults with AML/MDS before scaling to pediatric patients with SCID. The observed CL was faster in the SCID population relative to the AML/MDS population, which may be attributed to differences in age or disease state. Infants have higher rates of extravasation of plasma proteins due to proportionally larger capillary surface area per unit volume available for plasma protein exchange and larger "leaky" central organs with sinusoidal or fenestrated capillaries. FcRn expression in vascular endothelial cells may also increase with age (based on reverse-transcriptase polymerase chain reaction data in rats), but there is no consistent ontogeny pattern due to highly variable and conflicting data.[16,28] There is also limited information on the ontogeny of c-Kit. One study reported no significant difference in expression between normal adult and pediatric livers (1–13 years of age).[29] Another study in 1937 pediatric and adult patients with acute leukemia did not observe differences in the frequency of c-Kit–positive cases between adults and pediatric groups.[30] However, the SCID population in this study included older children, and there were minor differences by age (Figure S6), so the faster CL relative to the AML/MDS population is likely attributed to disease characteristics rather than age.

Severe combined immunodeficiency is a group of genetic disorders characterized by a block in T lymphocyte differentiation and abnormal development of other lymphocyte lineages such as B or natural killer lymphocytes or more rarely myeloid cells.[31,32] The pathogenesis of SCID reflects distinct molecular mechanisms that affect various stages of T cell development. During early T cell development, thymic lymphoid progenitor cells lacking CD4 or CD8 expression downregulate c-Kit expression during variability, diversity, and joining rearrangement to generate a functionally rearranged T cell receptor β chain.[33] Therefore, we hypothesize that c-Kit expression may be higher in the SCID population if T cell development is stunted, resulting in a greater proportion of pre–T cell receptors expressing c-Kit. However, this did not significantly impact the geometric mean fold ratios for JSP191 AUC_{∞} with 500 mg/kg IVIG, which were 0.75-fold versus 0.80-fold for c-Kit expressions of 457 and 1873 pmol/L, respectively. Other possibilities include greater internalization or degradation rates of the JSP191–c-Kit complex; faster nonspecific processes, including pinocytosis, lymphatic recycling, or catabolism by nonspecific proteases; or lower FcRn concentration in patients with SCID.

Per the FDA guidelines for interpreting DDI studies, clinically significant DDIs for a substrate drug can be determined based on (1) the concentration–response relationships from PK and pharmacodynamic analysis for the substrate drug (preferred method) or (2) if the 90% confidence intervals for systemic exposure ratios exceed the default no-effect boundary of 80%–125% in the absence of a clearly defined exposure–response relationship.[21] In this

study, the 90% confidence intervals for JSP191 in combination with IVIG at doses ≥500 mg/kg relative to JSP191 alone exceeded the default no-effect boundary of 80–125% and may be even greater for monoclonal antibodies lacking TMDD (Table S4). Based on a systemic review in 1218 patients with PI receiving IVIG treatment, the mean ± SD IVIG dose used in the 28 clinical studies ranged from 387 ± 88 to 560 ± 170 mg/kg every 3–4 weeks.[20] In another study using data collected from the Immunoglobulin Diagnosis, Evaluation, and key Learnings (IDEaL) Patient Registry, the average monthly dose of IVIG treatment was 472 mg/kg.[34] These finding suggest that IVIG treatment with monoclonal antibodies in patients with PI may result in a clinically significant DDI, depending on the IVIG dose administered and the exposure–response relationship for the specific monoclonal antibody.

The reported CL of IVIG in a randomized study in 30 healthy subjects with a mean (range) age of 26 (18–43) years receiving 600 mg/kg of different commercially available human immungolublin G products (a liquid formulation, a nanofiltered formulation, and an i.v. formulation Sandoglobulin® CSL/Novartis) was 4.69–4.76 ml/kg/day with half-lives ranging from 24 to 30 days that did not differ significantly by formulation.[35] In contrast, the reported mean IVIG CL across studies performed in patients with PI (mean ages from 8.0 to 42 years) ranged from 0.52 to 2.31 ml/kg/day, and the mean half-lives ranged from 25 to 44.6 days (Table S2). Similarly, the mean half-life of iodinated IgG was 38 days with 3.9% of the intravascular pool catabolized per day in patients with agammaglobulinemia compared with 22 days and 6.8%, respectively, in healthy individuals.[36] The specific mechanism for a decreased CL of IVIG in patients with PI relative to healthy subjects is unknown. Because the precise mechanism is unclear, we implemented this in the simulations by both decreasing the endosomal uptake to 0.13/min and by changing the endogenous plasma IgG concentrations to 660–1280 mg/dl.[20] Other possibilities include differences in recycling or FcRn concentrations.

In conclusion, we developed an adult and pediatric PBPK model for the monoclonal c-Kit antibody, JSP191, in combination with IVIG (300–2000 mg/kg) and predicted that IVIG treatment doses ≥500 mg/kg exceeded the default no-effect boundary of 80%–125% for JSP191. This finding suggests that IVIG treatment may result in reduced efficacy for some monoclonal antibodies administered in combination with moderate IVIG doses in patients with PI. A limitation of this study was that there were age or disease-related differences in JSP191 PK between patients with AML/MDS and SCID that were not clearly understood. We mechanistically accounted for these differences by increasing the c-Kit expression, but there is no literature data to our knowledge reporting c-Kit expression in healthy subjects or subjects with SCID. Interestingly, the CL for IVIG based on published studies was lower in patients with PI relative to healthy subjects (Table S2). A limitation is that we changed the rate constant for endosomal uptake for tesidolumab in adults with renal insufficiency and for IVIG plus JSP191 in patients with PI, which can limit the generalizability. Disease status can often impact monoclonal antibody nonspecific CL; however, the exact mechanism is poorly understood and thus not fully accounted for in the simulated disease populations. The subjects with PI in these studies primarily had common variable immunodeficiency and X-linked agglamaglobulinemia, which may differ from subjects with SCID. Further studies should be performed to characterize differences in PK of monoclonal antibodies relative to healthy subjects, such as differences in target expression or activity.

AUTHOR CONTRIBUTIONS

S.N.S. wrote the manuscript. S.N.S., R.D., and T.K. designed the research. S.N.S. performed the research. S.N.S., R.D., and T.K. analyzed the data.

ACKNOWLEDGMENTS

Paul Malik provided an example file and assisted with the incorporation of target-mediated drug disposition for JSP191 and c-Kit binding.

FUNDING

No funding was received for this work.

CONFLICT OF INTEREST

Sara N. Salerno and Tarundeep Kakkar are employees at Gilead and receive stock options. Rong Deng is a paid consultant for Gilead.

ORCID

Sara N. Salerno https://orcid.org/0000-0002-8884-2127

REFERENCES

1. Bayry J, Misra N, Latry V, et al. Mechanisms of action of intravenous immunoglobulins in autoimmune and inflammatory diseases. *Transfus Clin Biol*. 2003;10:165-169.
2. Roopenian DC, Akilesh S. FcRn: the neonatal Fc receptor comes of age. *Nat Rev Immunol*. 2007;7:715-725.
3. Hansen RJ, Balthasar JP. Effects of intravenous immunoglobulin on platelet count and antiplatelet antibody disposition in a rat model of immune thrombocytopenia. *Blood*. 2002;100:2087-2093.
4. Garg A, Balthasar JP. Physiologically-based pharmacokinetic (PBPK) model to predict IgG tissue kinetics in wild-type and FcRn-knockout mice. *J Pharmacokinet Pharmacodyn*. 2007;34:687-709.

5. Hansen RJ, Balthasar JP. Intravenous immunoglobulin mediates an increase in anti-platelet antibody clearance via the FcRn receptor. *Thromb Haemost*. 2002;88:898-907.
6. Jordan SC, Kucher K, Bagger M, et al. Intravenous immunoglobulin significantly reduces exposure of concomitantly administered anti-C5 monoclonal antibody tesidolumab. *Am J Transplant*. 2020;20:2581-2588.
7. Casteele NV, Oyamada J, Shimizu C, et al. Infliximab pharmacokinetics are influenced by intravenous immunoglobulin administration in patients with kawasaki disease. *Clin Pharmacokinet*. 2018;57:1593-1601.
8. Muffly L, Kwon HS, Chin M, et al. Phase 1 study of JSP191, an anti-CD117 monoclonal antibody, with low dose irradiation and fludarabine in older adults with MRD-positive AML/MDS undergoing allogeneic HCT. Transplant. Cell. Ther. Meet. 2021. Accessed February 11, 2021. http://www.jaspertherapeutics.com/wp-content/uploads/2021/08/TCT2021_MDS-AML-SUBMITTED-Poster.pdf
9. Muffly L, Kwon HS, Chin M, et al. Early results of phase 1 study of JSP191, an anti-CD117 monoclonal antibody, with non-myeloablative conditioning in older adults with MRD-positive MDS/AML undergoing allogenic hematopoietic cell transplantation. ASCO Annu. Meet. 2021. Accessed February 09, 2020. http://www.jaspertherapeutics.com/wp-content/uploads/2021/08/ASCO2021_AML_POSTER_SUBMITTED.pdf
10. Agarwal R, Dvorak CC, Moore TB, et al. Non-genotoxic anti-CD117 transplant conditioning in infants with newly diagnosed severe combined immune deficiency. Transplant. Cell. Ther Meet. 2021. Accessed February 09, 2020. https://www.jaspertherapeutics.com/wp-content/uploads/2021/02/TCT2021_SCID-SUBMITTED-Poster.pdf
11. Jasper Therapeutics Inc. Jasper therapeutics to present data on JSP191 conditioning in SCID patients at the 2021 American Society of Hematology Annual Meeting. Accessed February 09, 2020. https://ir.jaspertherapeutics.com/news-releases/news-release-details/jasper-therapeutics-present-data-jsp191-conditioning-scid
12. Open Systems Pharmacology Suite community. *Open Systems Pharmaology Suite Manual*, version 7.4. 2018. Accessed February 09, 2020. https://docs.open-systems-pharmacology.org/working-with-pk-sim/pk-sim-documentation
13. Niederalt C, Kuepfer L, Solodenko J, et al. A generic whole body physiologically based pharmacokinetic model for therapeutic proteins in PK-Sim. *J Pharmacokinet Pharmacodyn*. 2018;45:235-257.
14. Abcam. Rat IgG ELISA Kit. Accessed March 03, 2022. https://www.abcam.com/rat-igg-elisa-kit-ab189578.html
15. Salauze D, Serre V, Perrin C. Quantification of total IgM and IgG levels in rat sera by a sandwich ELISA technique. *Comp Haematol Int*. 1994;4:30-33.
16. Malik P, Edginton A. Integration of ontogeny into a physiologically based pharmacokinetic model for monoclonal antibodies in premature infants. *J Clin Pharmacol*. 2020;60(4):466-476.
17. Grifols Therapeutics LLC. Gamunex-C, immune globulin injection, 10% caprylate/chromatography purified. Full prescribing information. Accessed March 11, 2022. https://www.gamunex-c.com/documents/27482625/27482925/Gamunex-C+Prescribing+Information.pdf/9258bd0f-4205-47e1-ab80-540304c1ff8e
18. Meyer M, Schneckener S, Ludewig B, Kuepfer L, Lippert J. Using expression data for quantification of active processes in physiologically based pharmacokinetic modeling. *Drug Metab Dispos*. 2012;40:892-901.
19. Edginton AN, Schmitt W, Willmann S. Development and evaluation of a generic physiologically based pharmacokinetic model for children. *Clin Pharmacokinet*. 2006;45:1013-1034.
20. Lee JL, Mohamed Shah N, Makmor-Bakry M, et al. A systematic review and meta-regression analysis on the impact of increasing IgG trough level on infection rates in primary immunodeficiency patients on intravenous IgG therapy. *J Clin Immunol*. 2020;40:682-698.
21. U.S. Food and Drug Adminisration. Clinical drug interaction studies—Cytochrome P450 enzyme- and transporter-mediated drug interactions guidance for industry. 2020. Accessed March 11, 2022. https://www.fda.gov/regulatory-information/search-fda-guidance-documents/clinical-drug-interaction-studies-cytochrome-p450-enzyme-and-transporter-mediated-drug-interactions
22. Glassman PM, Balthasar JP. Physiologically-based modeling of monoclonal antibody pharmacokinetics in drug discovery and development. *Drug Metab Pharmacokinet*. 2019;34:3-13.
23. Zhou H, Sharma A. Therapeutic protein-drug interactions: plausible mechanisms and assessment strategies. *Expert Opin Drug Metab Toxicol*. 2016;12:1323-1331.
24. Machavaram KK, Almond LM, Rostami-Hodjegan A, et al. A physiologically based pharmacokinetic modeling approach to predict disease-drug interactions: suppression of CYP3A by IL-6. *Clin Pharmacol Ther*. 2013;94:260-268.
25. Jiang X, Zhuang Y, Xu Z, Wang W, Zhou H. Development of a physiologically based pharmacokinetic model to predict disease-mediated therapeutic protein-drug interactions: Modulation of multiple cytochrome P450 enzymes by interleukin-6. *AAPS J*. 2016;18:767-776.
26. Xu Y, Hijazi Y, Wolf A, Wu B, Sun YN, Zhu M. Physiologically based pharmacokinetic model to assess the influence of blinatumomab-mediated cytokine elevations on cytochrome P450 enzyme activity. *CPT Pharmacometrics Syst Pharmacol*. 2015;4:507-515.
27. Abdallah HM, Zhu AZX. A minimal physiologically-based pharmacokinetic model demonstrates role of the neonatal Fc receptor (FcRn) competition in drug–disease interactions with antibody therapy. *Clin Pharmacol Ther*. 2020;107:423-434.
28. Malik P, Edginton A. Pediatric physiology in relation to the pharmacokinetics of monoclonal antibodies. *Expert Opin Drug Metab Toxicol*. 2018;14(6):585-599.
29. Baumann U, Crosby HA, Ramani P, Kelly DA, Strain AJ. Expression of the stem cell factor receptor c-kit in normal and diseased pediatric liver: identification of a human hepatic progenitor cell? *Hepatology*. 1999;30:112-117.
30. Bene MC, Bernier M, Casasnovas RO, et al. The reliability and specificity of c-kit for the diagnosis of acute myeloid leukemias and undifferentiated leukemias. *Blood*. 1998;92:596-599.
31. Notarangelo LD. Primary immunodeficiencies. *J Allergy Clin Immunol*. 2010;125:S182-S194.
32. Fischer A. Severe combined immunodeficiencies (SCID). *Clin Exp Immunol*. 2000;122:143-149.
33. Michie AM, Zúñiga-Pflücker JC. Regulation of thymocyte differentiation: pre-TCR signals and β-selection. *Semin Immunol*. 2002;14:311-323.
34. Kearns S, Kristofek L, Bolgar W, Seidu L, Kile S. Clinical profile, dosing, and quality-of-life outcomes in primary immune

deficiency patients treated at home with immunoglobulin G: data from the IDEaL patient registry. *J Manag Care Spec Pharm*. 2017;23:400-406.
35. Andresen I, Kovarik JM, Spycher M, Bolli R. Product equivalence study comparing the tolerability, pharmacokinetics, and pharmacodynamics of various human immunoglobulin-G formulations. *J Clin Pharmacol*. 2000;40:722-730.
36. Waldmann TA, Strober W. Metabolism of immunoglobulins. *Prog Allergy*. 1969;13:1-110.
37. Malik P, Edginton AN. Physiologically-based pharmacokinetic modeling vs. allometric scaling for the prediction of infliximab pharmacokinetics in pediatric patients. *CPT Pharmacometrics Syst Pharmacol*. 2019;8(11):835-844.
38. Suzuki T, Ishii-Watabe A, Tada M, et al. Importance of neonatal FcR in regulating the serum half-life of therapeutic proteins containing the Fc domain of human IgG1: a comparative study of the affinity of monoclonal antibodies and Fc-fusion proteins to human neonatal FcR. *J Immunol*. 2010;184:1968-1976.
39. Yee N, Langen H, Besmer P. Mechanism of kit ligand, phorbol ester, and calcium-induced down-regulation of c-kit receptors in mast cells. *J Biol Chem*. 1993;268:14189-14201.

SUPPORTING INFORMATION

Additional supporting information can be found online in the Supporting Information section at the end of this article.

How to cite this article: Salerno SN, Deng R, Kakkar T. Physiologically-based pharmacokinetic modeling of immunoglobulin and antibody coadministration in patients with primary human immunodeficiency. *CPT Pharmacometrics Syst Pharmacol*. 2022;11:1316-1327. doi:10.1002/psp4.12847